Supplement of Biogeosciences, 16, 961–978, 2019
https://doi.org/10.5194/bg-16-961-2019-supplement

Biogeosciences
Open Access

Supplement of

Insights from year-long measurements of air–water CH_4 and CO_2 exchange in a coastal environment

Mingxi Yang et al.

Correspondence to: Mingxi Yang (miya@pml.ac.uk)

Derivation of 10-m neutral wind speed

Previous studies of wind distortion over a large superstructure such as a ship (e.g. Moat et al. 2005) suggest that wind flow might be accelerated upon encountering the Penlee headland. To account for this flow distortion effect, we used the concurrent wind speed measurements from the (assumed to be undistorted) L4 buoy (a PML-UK Met Office collaboration) over the 7.6 months when the buoy wind data were available. The mean ratio of PPAO wind speed to L4 wind speed was first computed in 5-degree wind direction bins. This mean ratio (about 1.1 for both air-water exchange sectors) was then used to correct the year-long PPAO wind speed data for flow distortion as a function of wind direction. The 10-m neutral wind speed (U_{10n}) is derived from the distortion-corrected Penlee winds using the COARE model (version 3.5; Edson et al. 2013).

Effect of rain on the eddy covariance (EC) greenhouse gas fluxes

Rain can add substantial noise to the measurement of wind velocities by sonic anemometers, especially at high frequencies, thereby increasing the uncertainty in the EC fluxes. In our case, the Gill R3 anemometer (used for the second half of the 1-year campaign) is much less affected by rain than the Windmaster Pro anemometer (used for the first half of the 1-year campaign) for the gas flux measurements. We have not filtered our gas fluxes by a threshold rain rate (e.g. a commonly used value is 1 mm/hr), but our quality control filtering that includes the noise level of the vertical wind velocity has removed most of the fluxes during rainy periods for the first half of the 1-year campaign. The second half of the 1-year campaign (when the R3 anemometer was used) retains more rainy periods. Where coincidental data were available, the mean wind velocities from the two sonic anemometers agreed to within 2%.

Would our annual mean gas fluxes be significantly biased by excluding most of the rainy periods? Over the entire year, hourly rain rate exceeded 1 mm/hr 7% of the time at PPAO when winds were from southwest. The average wind speed was about 50% higher during these rainy periods than during non-rainy periods. The Nightingale et al. (2000) wind speed relation predicts that the average K (and so flux magnitude) should be about 120% higher during these rainy periods than during non-rainy periods. Thus excluding fluxes during these rainy periods could result in an underestimation of the mean annual flux by approximately 8.4% (=0.07*1.2).

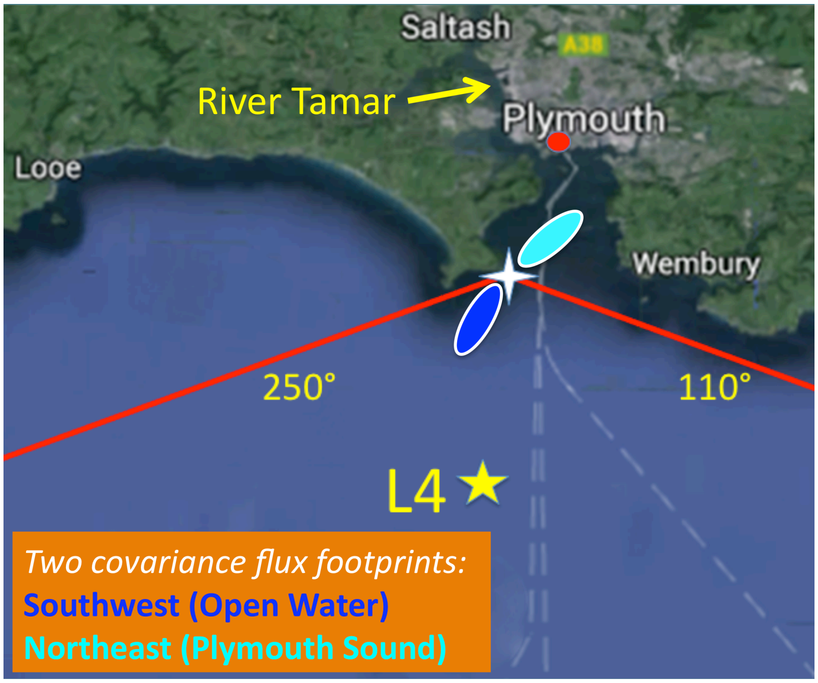

Figure S1. Map of study area. PPAO is indicated by the 4-point white star. L4 (yellow star) is 6 km south/southwest of PPAO. The approximate locations of the two eddy covariance air-water exchange footprints are shown: open water to the southwest, and Plymouth Sound to the northeast. Outflow from the river Tamar follows the western edge of the Plymouth Sound and wraps around the PPAO during ebbing tide.

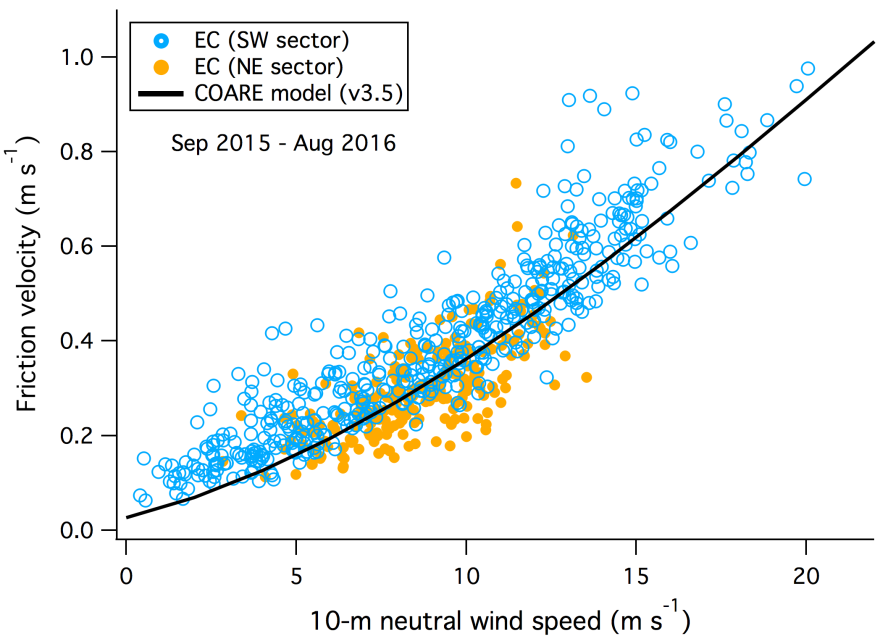

Figure S2. Friction velocity measured by eddy covariance vs. 10-m neutral wind speed (U10n) for the open water (southwest) and Plymouth (northeast) wind sectors.

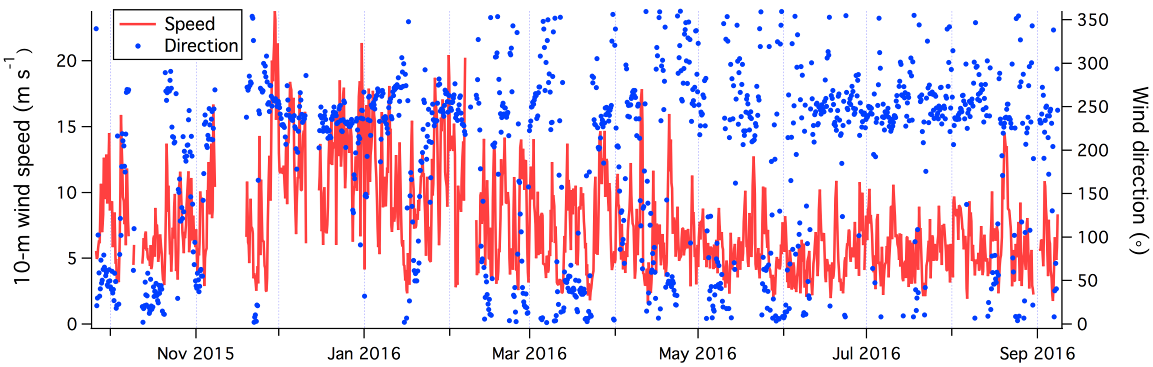

Figure S3. Time series of 10-m wind speed and wind direction at PPAO.

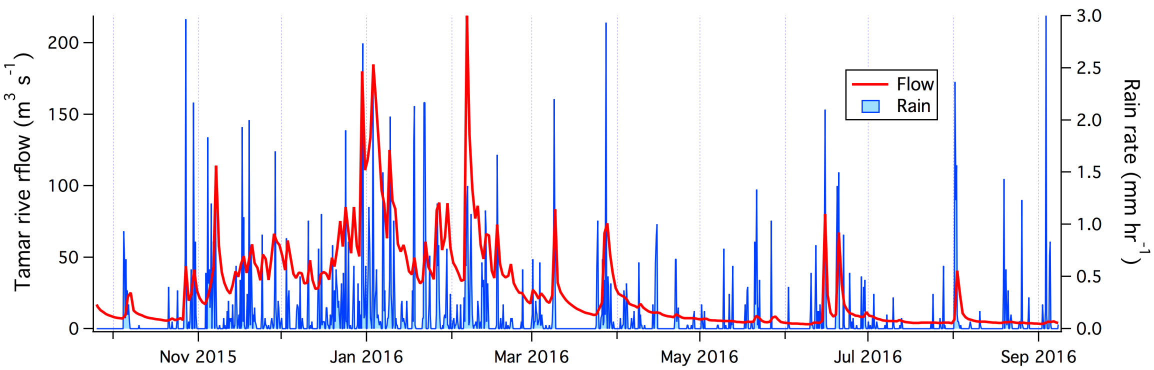

Figure S4. Time series of Tamar river flow (measured at Gunnislake) and rain rate.

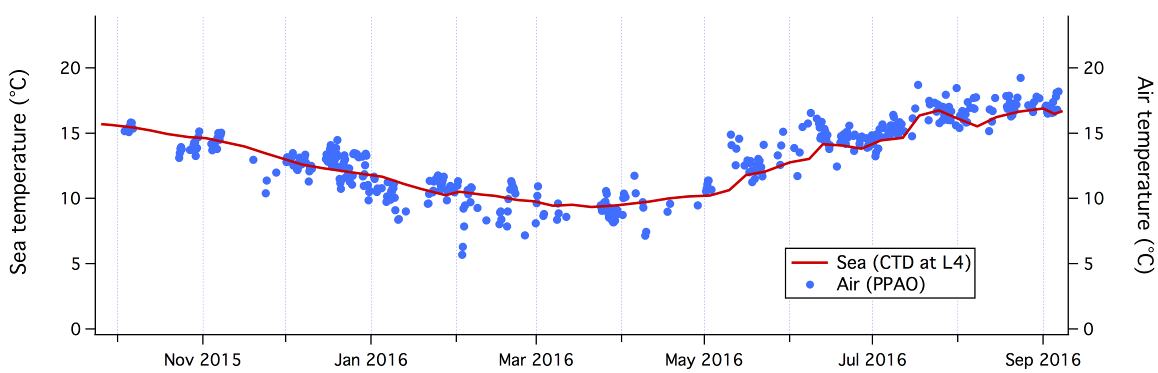

Figure S5. Time series of sea temperature at the L4 station (from CTD at 2 m depth) and air temperature at PPAO. Only air temperatures during southwesterly winds (open water sector) are shown.

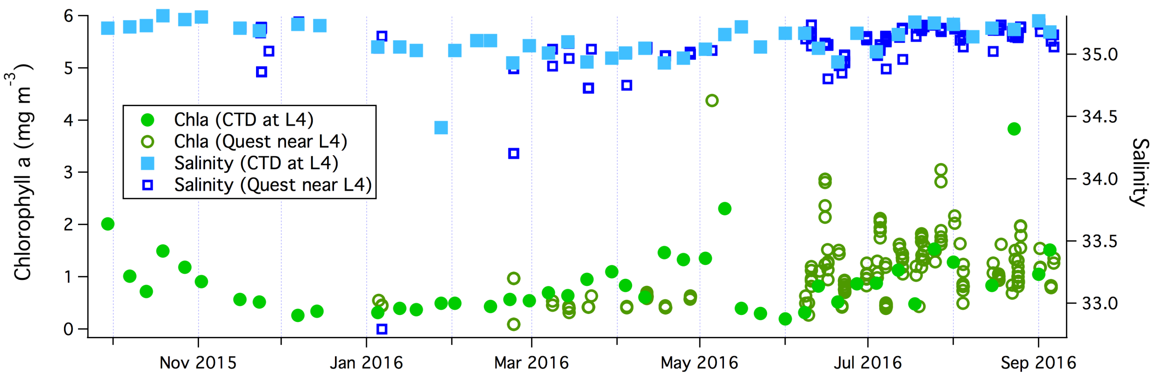

Figure S6. Time series of near surface chlorophyll a concentration and salinity, both from the CTD (2-m depth CTD cast) and from the RV Quest (underway fluorometer) at L4.

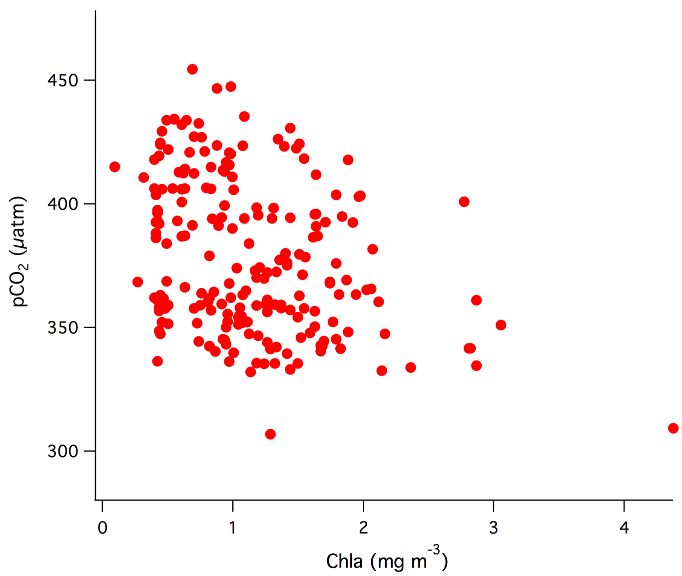

Figure S7. In situ pCO_2 broadly decreases with increasing Chla concentration.

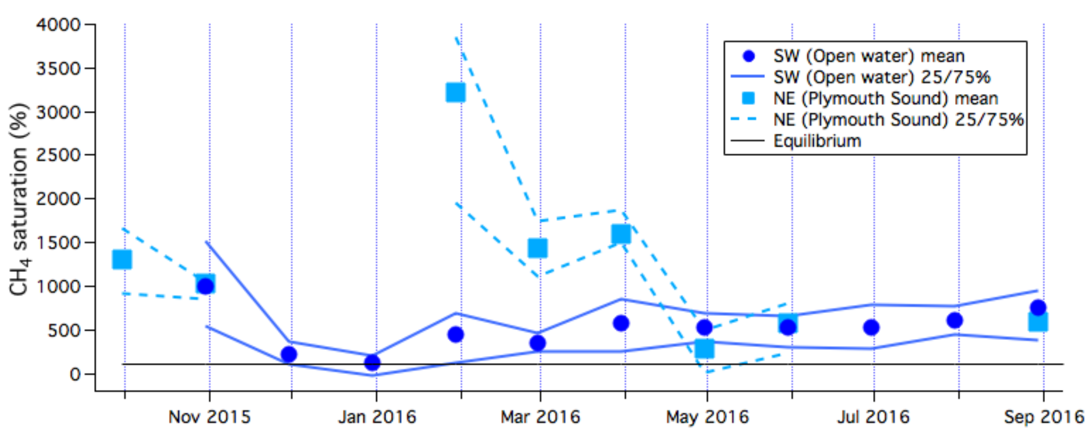

Figure S8. Monthly averages and 25/75 percentiles of implied CH_4 saturation in the surface waters within the EC flux footprint, along with the equilibrium value with respect to the atmosphere.

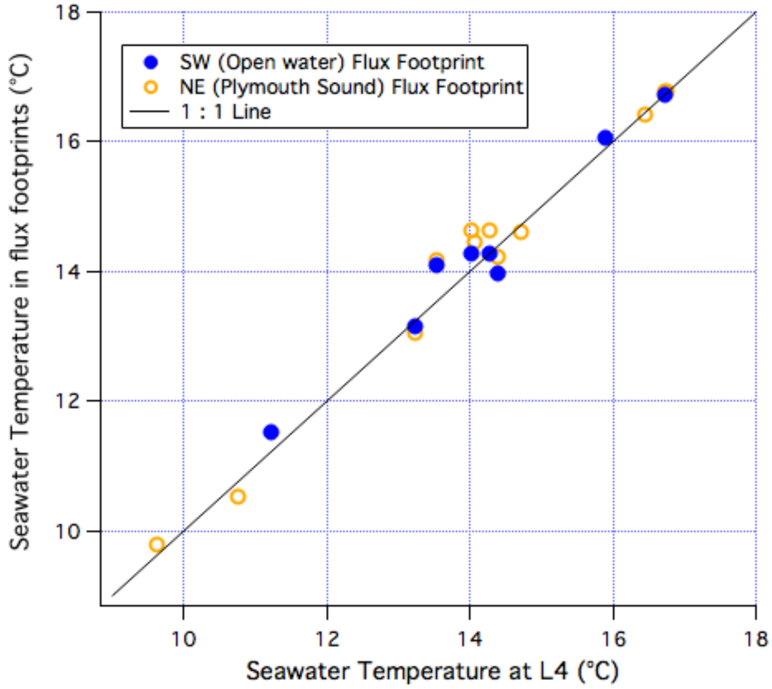

Figure S9. SST measured within the two PPAO air-water flux footprints vs. near-coincidental measurements from the *Quest* at the L4 station.

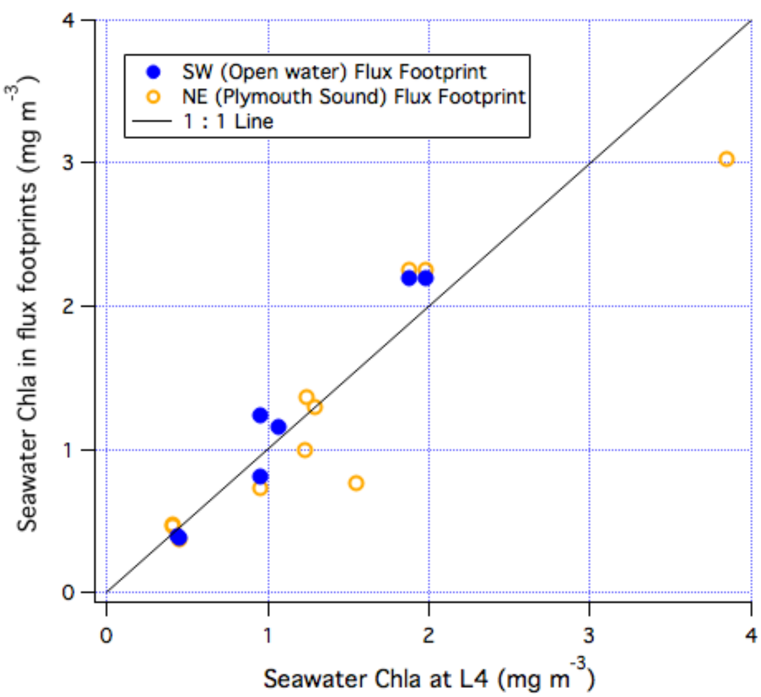

Figure S10. Chlorophyll a concentrations measured within the two PPAO air-water flux footprints vs. near-coincidental measurements from the *Quest* at the L4 station.

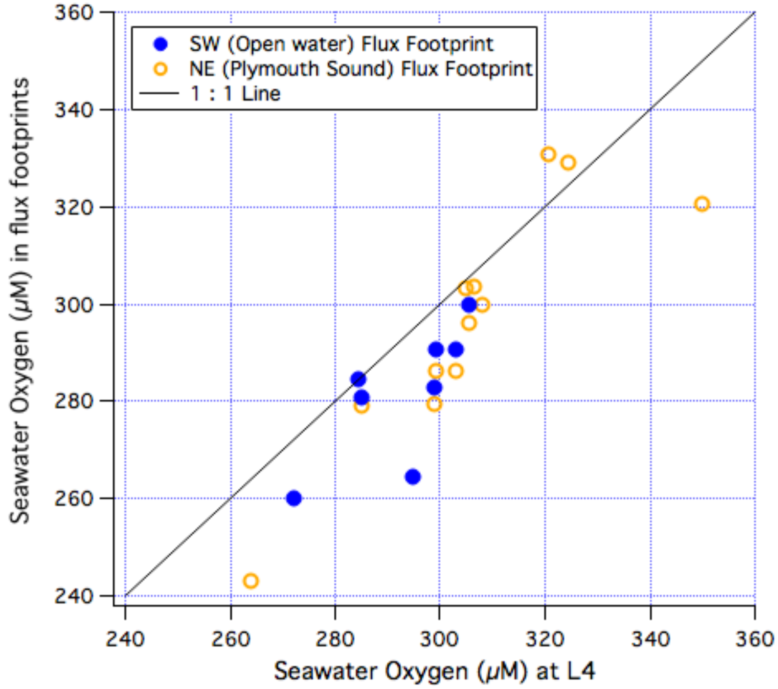

Figure S11. Dissolved oxygen measured within the two PPAO air-water flux footprints vs. near-coincidental measurements from the *Quest* at the L4 station.

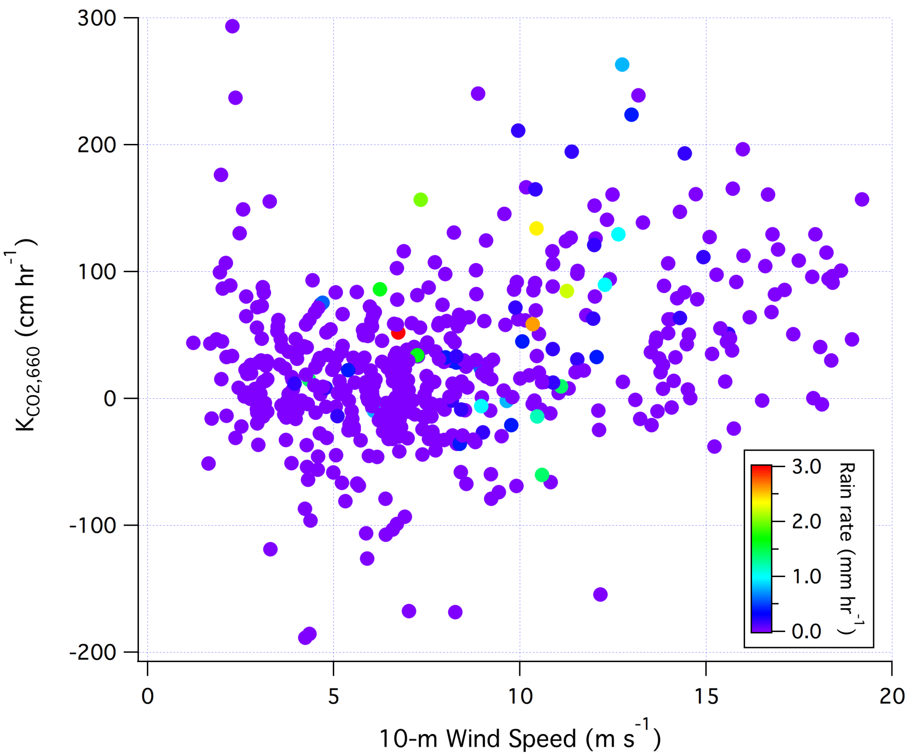

Figure S12. Hourly CO_2 transfer velocity (normalized to a Schmidt number of 660) vs. 10-m neutral wind speed for the southwest (open water) wind sector, color-coded by rain rate. At a given wind speed, rain does not appear to obviously enhance the gas transfer velocity.

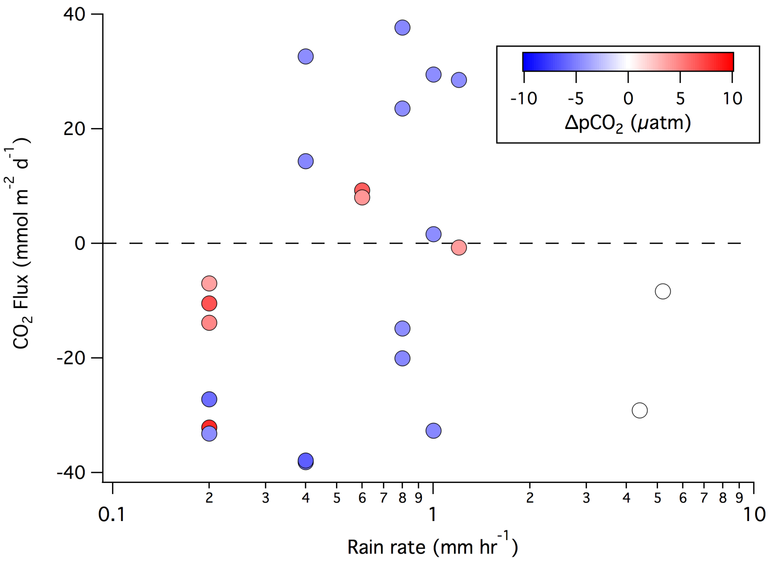

Figure S13. Hourly CO_2 flux vs. rain rate for the southwest (open water) wind sector, color-coded by the air-water CO_2 gradient. Data limited to periods when the absolute value of ΔpCO_2 was < 10 µatm. No obvious relationship is observed between CO_2 flux and rain rate. Mean CO_2 fluxes during these rainy periods were not significantly different from zero.

Edson, J. B., Jampana, V., Weller, R. A., Bigorre, S. P., Plueddemann, A. J., Fairall, C. W., Miller, S. D., Mahrt, L., Vickers, D., and Hersbach H.: On the exchange of momentum over the open ocean, J. Phys. Oceanogr., 43, 1589–1610, doi:10.1175/JPO-D-12-0173.1, 2013.

Moat, B.J., Yelland, M. J., Pascal, R. W., and Molland, A. F.: An overview of the airflow distortion at anemometer sites on ships. Int. J. Climatol., 25, 997–1006, 2005.